# GLOBAL CONSTRAINTS PRESERVING SCALAR AUXILIARY VARIABLE SCHEMES FOR GRADIENT FLOWS*

QING CHENG† AND JIE SHEN‡

**Abstract.** We develop several efficient numerical schemes which preserve exactly the global constraints for constrained gradient flows. Our schemes are based on the scalar auxiliary variable (SAV) approach combined with the Lagrangian multiplier approach. They are as efficient as the SAV schemes for unconstrained gradient flows, i.e., only require solving linear equations with constant coefficients at each time step plus an additional nonlinear algebraic system which can be solved at negligible cost, can be unconditionally energy stable, and preserves exactly the global constraints for constrained gradient flows. Ample numerical results for phase-field vesicle membrane and optimal partition models are presented to validate the effectiveness and accuracy of the proposed numerical schemes.

**1. Introduction.** Gradient flows are ubiquitous in science and engineering applications. In the last few decades, a large body of research has been devoted to developing efficient numerical schemes, particularly time discretization schemes, for gradient flows. We refer to the recent review paper [9] and the references therein, for a detailed account on these efforts; see also [21, 22] for a presentation of the newly developed invariant energy quadratization (IEQ) method [24, 26] and the scalar auxiliary method (SAV) method (cf. [20, 21, 7]) which have received much attention recently due to their efficiency, flexibility, and accuracy. However, most of the research in this area is concerned with unconstrained gradient flows. But many gradient flows in physical, chemical, and biological sciences are constrained with one or several global physical constraints, e.g., the norm of multicomponent wave functions is preserved in multicomponent Bose–Einstein condensates [2], the norm of each component is preserved in optimal eigenvalue partition problems [4, 8, 11], the stress is constrained to be negative in topology optimization problems [19, 15], the volume [16, 10] and surface area are preserved in the phase field vesicle membrane model [12, 23, 7, 14], and many others in constrained minimizations.

A highly desirable property of numerical algorithms for gradient flows with physical constraints is to be able to satisfy the energy dissipation law while preserving the physical constraints. But how to design numerical schemes which are energy stable while enforcing physical constraints, such as mass, norm, or surface area conservation, is a challenging task. A straightforward approach is to use the method of lines. Namely, first discretize the system in space, leading to a system of differential algebraic equations (DAEs), then use a suitable existing technique for DAEs (cf. [3, 1, 18] and the references therein) to solve it. A drawback of this approach is

†Department of Applied Mathematics, Illinois Institute of Technology, Chicago, IL 60616 (qcheng4@iit.edu).

‡Department of Mathematics, Purdue University, West Lafayette, IN 47907 (shen7@purdue.edu).

that for multi-dimensional problems, the size of the DAE system can be exceedingly large for the solver based on DAEs to be efficient. An alternative is first to construct a suitable discretization in time, then to use a Galerkin-type discretization in space so that nice properties of time discretization such as energy stability and constraint preserving can be carried over to the fully discretized schemes. In this paper, we shall concentrate on the time discretization. Two popular approaches to enforce constraints in a gradient system are the following:

- Penalty approach: add suitable penalty terms in the free energy and consider the unconstrained gradient flow with the new penalized free energy. Its advantage is that efficient numerical methods for unconstrained gradient flows can be directly applied, and in principle one can approximate the constraints to within arbitrary accuracy by choosing suitable penalty parameters. Its disadvantage is that large penalty parameters, which are needed for more accurate approximation of the constraints, may lead to very stiff systems that are difficult to solve efficiently. This approach is used in [23, 25, 7, 17] for the vesicle membrane model and in [27] for the multicomponent Bose–Einstein condensates.
- Lagrangian multiplier approach: introduce Lagrangian multipliers to enforce exactly the constraints. This approach is studied mathematically in [5] and numerically in [11] for the optimal eigenvalue partition problem. The main advantage is that the constraints can be satisfied exactly, while its drawback is that it will lead to difficulty in solving nonlinear systems at each time step.

The goal of this paper is to develop efficient time discretization for gradient flows with global constraints using the Lagrangian multiplier approach. To this end, we shall combine the SAV approach [21] with the Lagrangian multiplier approach [6], hoping to construct schemes which enjoy all advantages of the SAV schemes but can also preserve the constraints exactly using the Lagrangian multiplier approach with negligible additional cost. Three different approaches will be considered: (i) The first one is a direct combination of the SAV approach with the Lagrangian multiplier approach. The scheme is easy to implement but we are unable to prove that it is unconditionally energy stable. (ii) In the second approach, we replace the dynamic equation for the SAV by another Lagrangian multiplier so that the scheme becomes unconditionally energy stable, but leading to an additional coupled nonlinear algebraic system for the two Lagrangian multipliers to solve at each time step, instead of a nonlinear algebraic equation for just one Lagrangian multiplier in the first approach. (iii) In the third approach, we combine the advantages of the first two approaches to construct a scheme, which is unconditionally energy stable, such that the two Lagrangian multipliers can be determined sequentially, instead of a coupled system in the second approach. All three approaches have essentially the same computational cost as the linear SAV scheme, presented in section 2.1, which is extremely efficient and easy to implement but can only approximate the constraints up to the order of the scheme. Our numerical results indicate that the first and third approaches are generally more efficient and robust than the second approach.

The remainder of this paper is structured as follows. In section 2, we present a general methodology for gradient flows with one global constraint and propose three different approaches to devise efficient numerical schemes which can enforce exactly the constraint. In sections 3 and 4, we apply the general methodology introduced in section 2 to the phase field vesicle membrane model with two constraints and to the optimal partition model with multiple constraints, respectively. In section 5, we present numerical experiments to compare the performance of the three approaches

and the penalty approach and present several numerical simulations for the phase field vesicle membrane model with two constraints and to the optimal partition model with multiple constraints. Some concluding remarks are given in section 6.

**2. General methodology to preserve global constraints for gradient flows.** We present in this section a general methodology to preserve global constraints in gradient flows. To simplify the presentation, we consider here single-component gradient flows with a single global constraint. The approaches developed here will be extended to problems with multicomponents and multiglobal constraints in the subsequent sections.

To fix the idea, let $\Omega$ be a bounded domain in $\mathbb{R}^d$, $(\cdot, \cdot)$ be the inner product in $L^2(\Omega)$, and $\| \cdot \|$ be the associated norm in $L^2(\Omega)$. We also denote by $\| \cdot \|_k$ the usual Sobolev norm in $H^k(\Omega)$.

Let $F(\phi)$ be a nonlinear potential and $\mathcal{L}$ be a self-adjoint linear nonnegative operator in $L^2(\Omega)$, i.e.,

$$(2.1) \qquad < \mathcal{L}\phi, \phi >= (\mathcal{L}^{1/2}\phi, \mathcal{L}^{1/2}\phi) = \|\mathcal{L}^{1/2}\phi\|^2.$$

For example, $L = -\Delta$ with periodic or homogeneous Neumann boundary condition.

We consider the minimization of a total free energy in the form

$$(2.2) \qquad E(\phi) = \int_\Omega \frac{1}{2}\mathcal{L}\phi \cdot \phi + F(\phi)d\boldsymbol{x},$$

under a global constraint

$$(2.3) \qquad \frac{d}{dt}H(\phi) = 0 \ \text{ with } \ H(\phi) = \int_\Omega h(\phi)d\boldsymbol{x},$$

where $h(\phi)$ is a function of $\phi$.

This constrained minimization problem can be interpreted as the following gradient system with constraint [4, 11]:

$$(2.4) \qquad \begin{aligned} \phi_t &= -\mathcal{G}\left(\mathcal{L}\phi + F'(\phi) - \lambda(t)\frac{\delta H}{\delta \phi}\right), \\ \frac{d}{dt}H(\phi) &= 0, \end{aligned}$$

where $\lambda(t)$ is a Lagrange multiplier introduced to enforce the constraint, and $\mathcal{G}$ is a symmetric positive operator in $L^2(\Omega)$, i.e.,

$$(2.5) \qquad < \mathcal{G}\phi, \phi >= (\mathcal{G}^{1/2}\phi, \mathcal{G}^{1/2}\phi) = \|\mathcal{G}^{1/2}\phi\|^2,$$

describing the relaxation process of the system. For example, $\mathcal{G} = I$ represents the $L^2$ gradient flow while $\mathcal{G} = -\Delta$ with periodic or homogeneous Neumann boundary condition represents the $H^{-1}$ gradient flow.

Let us denote $\mu = \mathcal{L}\phi + F'(\phi) - \lambda(t)\frac{\delta H}{\delta \phi}$ and take its inner product with $-\phi_t$ on both sides, and sum up with the inner product of the first equation in (2.4) with $\mu$, we obtain the following energy dissipation law:

$$(2.6) \qquad \frac{d}{dt}E(\phi) = - < \mathcal{G}\mu, \mu >\leq 0.$$

We shall first construct a linear scheme based on the SAV approach which only approximates the global constraint, followed by three "essentially" linear schemes which enforce exactly the global constraint while retaining all essential advantages of the SAV approach.

**2.1. A linear scheme based on the SAV approach.** We start by constructing first a linear scheme based on the SAV approach for (2.4). Assuming $\int_\Omega F(\phi)d\boldsymbol{x} > -C_0$ for some $C_0 > 0$, we introduce a SAV $r(t) = \sqrt{\int_\Omega F(\phi)d\boldsymbol{x} + C_0}$ and rewrite (2.4) as

$$(2.7) \qquad\qquad \partial_t \phi = -\mathcal{G}\mu,$$

$$(2.8) \qquad\qquad \mu = \mathcal{L}\phi + \frac{r(t)}{\sqrt{\int_\Omega F(\phi)d\boldsymbol{x} + C_0}} F'(\phi) - \lambda \frac{\delta H}{\delta \phi},$$

$$(2.9) \qquad\qquad \frac{d}{dt}H(\phi) = 0,$$

$$(2.10) \qquad\qquad r_t = \frac{1}{2\sqrt{\int_\Omega F(\phi)d\boldsymbol{x} + C_0}}(F'(\phi), \phi_t).$$

Taking the inner products of the first two equations with $\mu$ and $-\phi_t$, respectively, summing up the results along with the fourth equation, and using the third equation, we obtain the following energy dissipation law:

$$(2.11) \qquad\qquad \frac{d}{dt}\tilde{E}(\phi) = -(\mathcal{G}\mu, \mu),$$

where $\tilde{E}(\phi) = \int_\Omega \frac{1}{2}\mathcal{L}\phi \cdot \phi d\boldsymbol{x} + r^2$ is a modified energy. Then, a first-order SAV scheme for the above modified system is

$$(2.12) \qquad \frac{\phi^{n+1} - \phi^n}{\delta t} = -\mathcal{G}\mu^{n+1},$$

$$(2.13) \qquad \mu^{n+1} = \mathcal{L}\phi^{n+1} + \frac{r^{n+1}}{\sqrt{\int_\Omega F(\phi^n)d\boldsymbol{x} + C_0}} F'(\phi^n) - \lambda^{n+1}\left(\frac{\delta H}{\delta \phi}\right)^n,$$

$$(2.14) \qquad \left(\left(\frac{\delta H}{\delta \phi}\right)^n, \phi^{n+1} - \phi^n\right) = 0,$$

$$(2.15) \qquad \frac{r^{n+1} - r^n}{\delta t} = \frac{1}{2\sqrt{\int_\Omega F(\phi^n)d\boldsymbol{x} + C_0}}\left(F'(\phi^n), \frac{\phi^{n+1} - \phi^n}{\delta t}\right).$$

As for the stability, we have the following result.

THEOREM 2.1. *The scheme* (2.12)–(2.15) *is unconditionally energy stable in the sense that*

$$\tilde{E}(\phi^{n+1}) - \tilde{E}(\phi^n) \leq -\Delta t(\mathcal{G}\mu^{n+1}, \mu^{n+1}),$$

*where* $\tilde{E}(\phi^k) = \int_\Omega \frac{1}{2}\mathcal{L}\phi^k \cdot \phi^k d\boldsymbol{x} + (r^k)^2$.

*Proof.* Taking the inner products of (2.12) with $\mu^{n+1}$ and of (2.13) with $-\frac{\phi^{n+1} - \phi^n}{\delta t}$, summing up the results, and taking into account (2.14)–(2.15), we obtain the desired result. $\qquad\square$

We now show that the above scheme can be efficiently implemented. Writing

$$(2.16) \quad \phi^{n+1} = \phi_1^{n+1} + \lambda^{n+1}\phi_2^{n+1}, \ \mu^{n+1} = \mu_1^{n+1} + \lambda^{n+1}\mu_2^{n+1}, \ r^{n+1} = r_1^{n+1} + \lambda^{n+1}r_2^{n+1}$$

in the above, we find that $(\phi_i^{n+1}, \mu_i^{n+1}, r_i^{n+1})$ $(i = 1, 2)$ can be determined as follows:

$$(2.17) \qquad \frac{\phi_1^{n+1} - \phi^n}{\delta t} = -\mathcal{G}\mu_1^{n+1},$$

$$(2.18) \qquad \mu_1^{n+1} = \mathcal{L}\phi_1^{n+1} + \frac{r_1^{n+1}}{\sqrt{\int_\Omega F(\phi^n)d\boldsymbol{x} + C_0}} F'(\phi^n),$$

$$(2.19) \qquad \frac{r_1^{n+1} - r^n}{\delta t} = \frac{1}{2\sqrt{\int_\Omega F(\phi^n)d\boldsymbol{x} + C_0}} \left( F'(\phi^n), \frac{\phi_1^{n+1} - \phi^n}{\delta t} \right);$$

and

$$(2.20) \qquad \frac{\phi_2^{n+1}}{\delta t} = -\mathcal{G}\mu_2^{n+1},$$

$$(2.21) \qquad \mu_2^{n+1} = \mathcal{L}\phi_2^{n+1} + \frac{r_2^{n+1}}{\sqrt{\int_\Omega F(\phi^n)d\boldsymbol{x} + C_0}} F'(\phi^n) - \left( \frac{\delta H}{\delta \phi} \right)^n,$$

$$(2.22) \qquad \frac{r_2^{n+1}}{\delta t} = \frac{1}{2\sqrt{\int_\Omega F(\phi^n)d\boldsymbol{x} + C_0}} \left( F'(\phi^n), \frac{\phi_2^{n+1}}{\delta t} \right).$$

Since $r_i^{n+1}$ $(i = 1, 2)$ is just a constant which can be easily eliminated by using a block Gaussian elimination, each of the above solutions can be obtained by solving two linear systems with constant coefficients of the form (cf. [21] for more detail):

$$(2.23) \qquad \begin{pmatrix} \frac{1}{\Delta t}I & \mathcal{G} \\ \mathcal{L} & -I \end{pmatrix} \begin{pmatrix} \phi \\ \mu \end{pmatrix} = \bar{b}.$$

Once we determine $(\phi_i^{n+1}, \mu_i^{n+1}, r_i^{n+1})$ $(i = 1, 2)$ from the above, we use (2.14) to determine $\lambda^{n+1}$ explicitly by

$$(2.24) \qquad \lambda^{n+1} = - \left( \left( \frac{\delta H}{\delta \phi} \right)^n, \phi_1^{n+1} - \phi^n \right) \Big/ \left( \left( \frac{\delta H}{\delta \phi} \right)^n, \phi_2^{n+1} \right).$$

Hence, the scheme is very efficient. However, the global constraint (2.9) is only approximated to first-order. While we can easily construct second-order energy stable SAV schemes which approximate (2.9) to second-order, we cannot preserve (2.9) exactly. Below, we show how to modify the scheme (2.12)–(2.15) so that we can preserve (2.9) exactly while keeping its essential advantages.

**2.2. The first approach.** The first approach is simply to replace the first order approximation of (2.14) by enforcing exactly (2.9). More precisely, a modified first-order scheme is as follows:

$$(2.25) \qquad \frac{\phi^{n+1} - \phi^n}{\delta t} = -\mathcal{G}\mu^{n+1},$$

$$(2.26) \qquad \mu^{n+1} = \mathcal{L}\phi^{n+1} + \frac{r^{n+1}}{\sqrt{\int_\Omega F(\phi^n)d\boldsymbol{x} + C_0}} F'(\phi^n) - \lambda^{n+1} \left( \frac{\delta H}{\delta \phi} \right)^n,$$

$$(2.27) \qquad H(\phi^{n+1}) = H(\phi^0),$$

$$(2.28) \qquad \frac{r^{n+1} - r^n}{\delta t} = \frac{1}{2\sqrt{\int_\Omega F(\phi^n)d\boldsymbol{x} + C_0}} \left( F'(\phi^n), \frac{\phi^{n+1} - \phi^n}{\delta t} \right).$$

The above scheme can be implemented in essentially the same procedure as the scheme (2.12)–(2.15). Indeed, still writing $(\phi^{n+1}, \mu^{n+1})$ as in (2.16), we can still determine $(\phi_i^{n+1}, \mu_i^{n+1}, i = 1, 2)$ from (2.17)–(2.19) and (2.20)–(2.22). The only difference is that we now need to determine $\lambda^{n+1}$ from (2.27) which leads to a nonlinear algebraic equation for $\lambda^{n+1}$:

$$(2.29) \qquad (h(\phi_1^{n+1} + \lambda^{n+1}\phi_2^{n+1}) - h(\phi^n), 1) = 0.$$

*Remark* 2.1. The complexity of this nonlinear algebraic equation depends on $h(\phi)$. For example, if $h(\phi) = \phi^2$ as in some applications, it will be a quadratic equation so it can be solved directly and exactly using the quadratic formula. For more complicated $h(\phi)$, the nonlinear algebraic equation (2.29) here, and in other schemes to be presented, can be solved by a standard Newton iteration. It is well-known that the convergence of the Newton iteration depends on a good initial guess. We can use the linear scheme (2.12)–(2.15) to produce a good and reliable initial guess so that the Newton iteration will converge very quickly with negligible cost. Hence, the system (2.25)–(2.28) is "essentially" linear as it involves a linear system plus a nonlinear algebraic equation and can be efficiently solved.

Next, we examine the stability of scheme (2.25)–(2.28).

PROPOSITION 2.1. *Let* $\{\phi^k, \mu^k, \lambda^k, r^k\}$ *be a solution of the scheme* (2.25)–(2.28). *Then, the following energy law is satisfied unconditionally for all* $n$:

$$(2.30) \quad \tilde{E}^{n+1} - \tilde{E}^n + \frac{\lambda^{n+1}}{2}(h''(\xi^n)(\phi^{n+1} - \phi^n), \phi^{n+1} - \phi^n) \leq -\delta t(\mathcal{G}\mu^{n+1}, \mu^{n+1}),$$

*where*

$$\tilde{E}^n = \frac{1}{2}(\mathcal{L}\phi^n, \phi^n) + (r^n)^2.$$

*Proof.* Taking the inner products of (2.25) with $\mu^{n+1}$, of (2.26) with $-\frac{\phi^{n+1} - \phi^n}{\delta t}$, and of (2.27) with $2r^{n+1}$, summing up the results, we obtain

$$(2.31) \quad \begin{aligned} &\frac{1}{2\delta t}\left\{(\mathcal{L}\phi^{n+1}, \phi^{n+1}) - (\mathcal{L}\phi^n, \phi^n) + (\mathcal{L}(\phi^{n+1} - \phi^n), \phi^{n+1} - \phi^n)\right\} \\ &\qquad + \frac{1}{\delta t}\{(r^{n+1})^2 - (r^n)^2 + (r^{n+1} - r^n)^2\} \\ &= -(\mathcal{G}\mu^{n+1}, \mu^{n+1}) + \lambda^{n+1}\left(\left(\frac{\delta H}{\delta\phi}\right)^n, \frac{\phi^{n+1} - \phi^n}{\delta t}\right). \end{aligned}$$

By Taylor expansion, we have
$$(2.32)$$
$$(h(\phi^{n+1}), 1) - (h(\phi^n), 1) = \left(\left(\frac{\delta H}{\delta\phi}\right)^n, \phi^{n+1} - \phi^n\right) + \frac{1}{2}(h''(\xi^n)(\phi^{n+1} - \phi^n), \phi^{n+1} - \phi^n).$$

We can then conclude from the above two relations. $\qquad\square$

*Remark* 2.2. Assuming $h''(\phi) \geq 0$ for all $\phi$, then if $\lambda^{n+1} \geq 0$ for all $n$, the above result indicates that the scheme (2.25)–(2.28) is unconditionally energy dissipative. Note that for some applications, we have $h''(\phi) \geq 0$ and one can show that $\lambda(t) > 0$ (cf. [5]). But we are unable to show in general $\lambda^{n+1} \geq 0$ for all $n$. However, our numerical results indicate that this is true at least for the examples we consider in this paper.

**2.3. The second approach.** The main drawback of the first approach is that we cannot rigorously prove that the scheme is energy dissipative. We present below an approach which is as efficient as the first approach but is energy stable. The key idea is to introduce another Lagrange multiplier $\eta(t)$ to enforce the energy dissipation. More precisely, we rewrite (2.7)–(2.10) as follows:

$$\partial_t\phi = -\mathcal{G}\mu, \tag{2.33}$$

$$\mu = \mathcal{L}\phi + \eta(t)F'(\phi) - \lambda(t)\frac{\delta H}{\delta\phi}, \tag{2.34}$$

$$\frac{d}{dt}\int_\Omega h(\phi)d\boldsymbol{x} = 0, \tag{2.35}$$

$$\frac{d}{dt}\int_\Omega F(\phi)d\boldsymbol{x} = \eta(t)(F'(\phi),\phi_t) - \lambda(t)\left(\frac{\delta H}{\delta\phi},\phi_t\right). \tag{2.36}$$

Note that the last term in (2.36) is zero thanks to (2.35). We added this zero term here for the sake of constructing energy stable schemes below.

Taking the inner products of the first two equations with $\mu$ and $-\phi_t$, respectively, summing up the results along with the fourth equation, and using the third equation, we obtain the following energy dissipation law:

$$\frac{d}{dt}E(\phi) = -(\mathcal{G}\mu,\mu), \tag{2.37}$$

where $E(\phi)$ is the original energy defined in (2.2).

For example, a second-order scheme based on Crank–Nicolson can be constructed as follows:

$$\frac{\phi^{n+1} - \phi^n}{\delta t} = -\mathcal{G}\mu^{n+1/2}, \tag{2.38}$$

$$\mu^{n+1/2} = \mathcal{L}\phi^{n+1/2} + \eta^{n+1/2}F'(\phi^{*,n+1/2}) - \lambda^{n+1/2}\left(\frac{\delta H}{\delta\phi}\right)^{*,n+1/2}, \tag{2.39}$$

$$H(\phi^{n+1}) = H(\phi^0), \tag{2.40}$$

$$\int_\Omega F(\phi^{n+1}) - F(\phi^n)d\boldsymbol{x} = \eta^{n+1/2}(F'(\phi^{*,n+1/2}),\phi^{n+1} - \phi^n) \tag{2.41}$$
$$- \lambda^{n+1/2}\left(\left(\frac{\delta H}{\delta\phi}\right)^{*,n+1/2},\phi^{n+1} - \phi^n\right),$$

where $f^{n+1/2} = \frac{1}{2}(f^{n+1} + f^n)$ and $f^{*,n+1/2} = \frac{1}{2}(3f^n - f^{n-1})$ for any sequence $\{f^n\}$. Note that unlike in the continuous case, the last term in (2.41) is no longer zero; it is a second-order approximation to zero. This term is necessary for the unconditional stability stated below.

THEOREM 2.2. *Let $\{\phi^k,\mu^k,\lambda^k,\eta^k\}$ be a solution of the scheme* (2.38)–(2.41). *Then, the following energy law is satisfied unconditionally for all $n$:*

$$E(\phi^{n+1}) - E(\phi^n) = -\delta t(\mathcal{G}\mu^{n+1/2},\mu^{n+1/2}),$$

*where $E(\phi)$ is the original energy defined in* (2.2).

*Proof.* Taking the inner products of (2.38) with $\mu^{n+1/2}$ and of (2.39) with $-\frac{\phi^{n+1}-\phi^n}{\delta t}$, summing up the results along with (2.41), we immediately derive the desired results. $\square$

The above scheme can be efficiently implemented as the previous two schemes. Indeed, writing

(2.42)
$$\phi^{n+1} = \phi_1^{n+1} + \eta^{n+1/2}\phi_2^{n+1} + \lambda^{n+1/2}\phi_3^{n+1}, \ \mu^{n+1} = \mu_1^{n+1} + \eta^{n+1/2}\mu_2^{n+1} + \lambda^{n+1/2}\mu_3^{n+1}$$

in the scheme (2.38)–(2.41), we find that $(\phi_i^{n+1}, \mu_i^{n+1})$ $(i = 1, 2, 3)$ can be determined as follows:

$$(2.43) \qquad \frac{\phi_1^{n+1} - \phi^n}{\delta t} = -\mathcal{G}\mu_1^{n+1/2},$$

$$(2.44) \qquad \mu_1^{n+1/2} = \mathcal{L}\phi_1^{n+1/2};$$

$$(2.45) \qquad \frac{\phi_2^{n+1}}{\delta t} = -\mathcal{G}\mu_2^{n+1/2},$$

$$(2.46) \qquad \mu_2^{n+1/2} = \mathcal{L}\phi_2^{n+1/2} + F'(\phi^{*,n+1/2});$$

and

$$(2.47) \qquad \frac{\phi_3^{n+1}}{\delta t} = -\mathcal{G}\mu_3^{n+1/2},$$

$$(2.48) \qquad \mu_3^{n+1/2} = \mathcal{L}\phi_3^{n+1/2} - \left(\frac{\delta H}{\delta \phi}\right)^{*,n+1/2}.$$

The above three linear systems with constant coefficients can be easily solved. Once we determine $(\phi_i^{n+1}, \mu_i^{n+1})$ $(i = 1, 2, 3)$ from the above, it remains to solve for $(\eta^{n+1/2}, \lambda^{n+1/2})$. To this end, we plug (2.42) into (2.40) and (2.41), leading to a coupled nonlinear algebraic system for $(\eta^{n+1/2}, \lambda^{n+1/2})$. The complexity of this non-linear algebraic equation depends on $F(\phi)$ and $h(\phi)$.

*Remark* 2.3. The coupled nonlinear algebraic system for $(\eta^{n+1/2}, \lambda^{n+1/2})$ can be solved by Newton iteration. Since the exact solution for $\eta(t)$ is $\eta(t) \equiv 1$, we can use 1 as the initial guess for $\eta^{n+1/2}$, and still use the linear scheme (2.12)–(2.15), or its second-order version based on Crank–Nicolson, to produce an initial guess for $\lambda^{n+1/2}$. With this set of initial guesses, the Newton iteration for the coupled nonlinear algebraic system would converge quickly if $\Delta t$ is not too large.

**2.4. The third approach.** In the second approach, one needs to solve a coupled nonlinear algebraic system for $(\lambda^{n+1/2}, \eta^{n+1/2})$. The Newton's iteration may fail to converge if $\delta t$ is not sufficiently small. We propose below a modified version in which one can solve $\lambda^{n+1/2}$ first as in the first approach and then determine $\eta^{n+1/2}$ from a nonlinear algebraic equation:

$$(2.49) \qquad \frac{\phi^{n+1} - \phi^n}{\delta t} = -\mathcal{G}\mu^{n+1/2},$$

$$(2.50) \qquad \mu^{n+1/2} = \mathcal{L}\phi^{n+1/2} + \eta^{n+1/2}F'(\phi^{*,n+1/2}) - \lambda^{n+1/2}\left(\frac{\delta H}{\delta \phi}\right)^{*,n+1/2},$$

$$(2.51) \qquad H(\bar{\phi}^{n+1}) = H(\bar{\phi}^0),$$

$$(2.52) \qquad \int_\Omega F(\phi^{n+1}) - F(\phi^n)d\boldsymbol{x} = \eta^{n+1/2}(F'(\phi^{*,n+1/2}), \phi^{n+1} - \phi^n)$$
$$- \lambda^{n+1/2}\left(\left(\frac{\delta H}{\delta \phi}\right)^{*,n+1/2}, \phi^{n+1} - \phi^n\right),$$

where $f^{n+1/2} = \frac{1}{2}(f^{n+1} + f^n)$ and $f^{*,n+1/2} = \frac{1}{2}(3f^n - f^{n-1})$ for any sequence $\{g^n\}$, and $\bar{\phi}^{n+1}$ is defined as follows: Writing $(\phi^{n+1}, \mu^{n+1})$ as in (2.42) and plugging in (2.49)–(2.50), we can determine $(\phi_i^{n+1}, i = 1, 2, 3)$ (2.43)–(2.44), (2.45)–(2.46), and (2.47)–(2.48) respectively. Then, we set $\bar{\phi}^{n+1} = \phi_1^{n+1} + \phi_2^{n+1} + \lambda^{n+1/2}\phi_3^{n+1}$.

*Remark* 2.4. The only difference between the above scheme and the scheme (2.38)–(2.41) is that $\phi^{n+1}$ in (2.40) is replaced by $\bar{\phi}^{n+1}$ in (2.51) which is independent of $\eta^{n+1/2}$. This is reasonable since $\eta^{n+1/2}$ is an approximation of 1. As a consequence, $\lambda^{n+1/2}$ and $\eta^{n+1/2}$ can be decoupled as shown below.

The scheme (2.49)–(2.52) can be efficiently implemented as follows:
- Solve $(\phi_i^{n+1}, \mu_i^{n+1}, i = 1, 2, 3)$ from (2.43)–(2.44), (2.45)–(2.46), and (2.47)–(2.48).
- Determine $\lambda^{n+1/2}$ from (2.51). This is a nonlinear algebraic equation for $\lambda^{n+1/2}$, so it can be solved with Newton iteration by using the linear scheme (2.12)–(2.15), or its second-order version based on Crank–Nicolson, to produce an initial guess for $\lambda^{n+1/2}$.
- With $\lambda^{n+1/2}$ known, plugging $\phi^{n+1} = \phi_1^{n+1} + \eta^{n+1/2}\phi_2^{n+1} + \lambda^{n+1/2}\phi_3^{n+1}$ into (2.52) leads to a nonlinear algebraic equation for $\eta^{n+1/2}$ which can be solved by a Newton iteration with $\eta^{n+1/2} = 1$ as the initial condition.
- Finally we obtain $(\phi^{n+1}, \mu^{n+1})$ through (2.42).

As for the scheme (2.38)–(2.41), we can easily establish the following result.

THEOREM 2.3. *Let $\{\phi^k, \mu^k, \lambda^k, \eta^k\}$ be a solution of the scheme (2.49)–(2.52). Then, the following energy law is satisfied unconditionally for all $n$:*

$$E(\phi^{n+1}) - E(\phi^n) = -\delta t(\mathcal{G}\mu^{n+1/2}, \mu^{n+1/2}),$$

*where $E(\phi)$ is the original energy defined in (2.2).*

*Proof.* Taking the inner products of (2.49) with $\mu^{n+1/2}$ and of (2.50) with $-\frac{\phi^{n+1} - \phi^n}{\delta t}$, summing up the results along with (2.52), we immediately derive the desired results. □

**2.5. Stabilization and adaptive time stepping.** For problems with stiff nonlinear terms, one may have to use very small time steps to obtain accurate results with any of the three approaches above. In order to allow larger time steps while achieving desired accuracy, we may add suitable stabilization and use adaptive time stepping.

**2.5.1. Stabilization.** Instead of solving (2.4), we consider a perturbed system with two additional stabilization terms,

$$\phi_t = -\mathcal{G}\mu,$$

(2.53)
$$\mu = \mathcal{L}\phi + \epsilon_1\phi_{tt} + \epsilon_2\mathcal{L}\phi_{tt} + F'(\phi) - \lambda\frac{\delta H}{\delta\phi},$$

$$\frac{d}{dt}H(\phi) = 0,$$

where $\epsilon_i$, $i = 1, 2$, are two small stabilization constants whose choices will depend on how stiff the nonlinear terms are. It is easy to see that the above system is a gradient flow with a perturbed free energy $E_\epsilon(\phi) = E(\phi) + \frac{\epsilon_1}{2}(\phi_t, \phi_t) + \frac{\epsilon_2}{2}(\mathcal{L}\phi_t, \phi_t)$ and satisfies the following energy law:

(2.54)
$$\frac{d}{dt}E_\epsilon(\phi) = -(\mathcal{G}\mu, \mu).$$

The schemes presented before for (2.4) can all be easily extended for (2.53) while keeping the same simplicity. For example, a second-order scheme based on the second approach is

$$(2.55) \qquad \frac{\phi^{n+1} - \phi^n}{\delta t} = -\mathcal{G}\mu^{n+1/2},$$

$$(2.56) \qquad \mu^{n+1/2} = \mathcal{L}\phi^{n+1/2} + \frac{\epsilon_1}{(\delta t)^2}(\phi^{n+1} - 2\phi^n + \phi^{n-1})$$

$$(2.57) \qquad\qquad + \frac{\epsilon_2}{(\delta t)^2}\mathcal{L}(\phi^{n+1} - 2\phi^n + \phi^{n-1})$$

$$+ \eta^{n+1/2}F'(\phi^{*,n+1/2}) - \lambda^{n+1/2}\left(\frac{\delta H}{\delta \phi}\right)^{*,n+1/2},$$

$$(2.58) \qquad H(\phi^{n+1}) = H(\phi^0),$$

$$(2.59) \qquad \int_\Omega F(\phi^{n+1}) - F(\phi^n)d\boldsymbol{x} = \eta^{n+1/2}(F'(\phi^{*,n+1/2}), \phi^{n+1} - \phi^n)$$

$$- \lambda^{n+1/2}\left(\left(\frac{\delta H}{\delta \phi}\right)^{*,n+1/2}, \phi^{n+1} - \phi^n\right),$$

where $f^{n+1/2} = \frac{1}{2}(f^{n+1} + f^n)$ and $f^{*,n+1/2} = \frac{1}{2}(3f^n - f^{n-1})$ for any sequence $\{f^n\}$.

THEOREM 2.4. *Let $\{\phi^k, \mu^k, \lambda^k, \eta^k\}$ be a solution of the scheme* (2.55)–(2.59). *Then, the following energy law is satisfied unconditionally for all n:*

$$E_\epsilon^{n+1} - E_\epsilon^n \leq -\delta t(\mathcal{G}\mu^{n+1/2}, \mu^{n+1/2}),$$

*where $E_\epsilon^k = E(\phi^k) + \frac{\epsilon_1}{2}\left(\frac{\phi^k - \phi^{k-1}}{\delta t}, \frac{\phi^k - \phi^{k-1}}{\delta t}\right) + \frac{\epsilon_2}{2}\left(\mathcal{L}\frac{\phi^k - \phi^{k-1}}{\delta t}, \frac{\phi^k - \phi^{k-1}}{\delta t}\right)$ with $E(\phi)$ being the original free energy defined in* (2.2).

*Proof.* Taking the inner products of (2.55) with $\mu^{n+1/2}$ and of (2.57) with $-\frac{\phi^{n+1} - \phi^n}{\delta t}$, summing up the results along with (2.59), and dropping some unnecessary terms, we immediately derive the desired results. $\square$

It is clear that the above scheme can be efficiently implemented as the scheme (2.38)–(2.41).

**2.6. Adaptive time stepping.** A main advantage of unconditionally stable schemes, such as the schemes using the second and third approaches, is that one can choose time steps solely based on the accuracy requirement. Hence, a suitable adaptive time stepping can greatly improve the efficiency. There are many different strategies for adaptive time stepping; we refer to [21] for some simple strategies which have proven to be effective for the SAV related approaches.

**3. A single-component system with multiple constraints.** The three approaches presented in the last section can be easily extended to gradient flows with multicomponents and/or multiglobal constraints. We consider in this section a single-component system with two global constraints.

**3.1. The model.** Vesicle membranes are formed by lipid bilayers which play an essential role in biological functions and its equilibrium shapes often characterized by bending energy and two physical constraints as described below.

As in [13, 12, 7], we consider the bending energy

$$(3.1) \qquad E_b(\phi) = \frac{\epsilon}{2}\int_\Omega \left(-\Delta\phi + \frac{1}{\epsilon^2}G(\phi)\right)^2 d\boldsymbol{x} = \frac{\epsilon}{2}\int_\Omega w^2 d\boldsymbol{x},$$

where

$$w := -\Delta\phi + \frac{1}{\epsilon^2}G(\phi), \quad G(\phi) := F'(\phi),\ F(\phi) = \frac{1}{4}(\phi^2 - 1)^2.$$

In the above, the level set $\{\phi(\boldsymbol{x}, t) = 0\}$ denotes the vesicle membrane surface, while $\{\phi(\boldsymbol{x}, t) > 0\}$ and $\{\phi(\boldsymbol{x}, t) < 0\}$ represent the inside and outside of the membrane surface, respectively, and $\epsilon$ is width of transition layer.

During the evolution, the membranes also preserve total volume and surface area represented by

$$(3.2) \quad A(\phi) = \int_\Omega \phi d\boldsymbol{x} \quad and \quad H(\phi) = \int_\Omega h(\phi)d\boldsymbol{x} \ \ with \ \ h(\phi) = \frac{\epsilon}{2}|\nabla\phi|^2 + \frac{1}{\epsilon}F(\phi).$$

We now introduce two Lagrange multipliers, $\gamma(t)$ and $\lambda(t)$, to enforce the volume and surface area conservations. The corresponding gradient flow reads

$$(3.3) \qquad\qquad \phi_t = -M\mu,$$

$$(3.4) \qquad\qquad \mu = -\epsilon\Delta w + \frac{1}{\epsilon}G'(\phi)w + \gamma(t) + \lambda(t)\frac{\delta H}{\delta\phi},$$

$$(3.5) \qquad\qquad w = -\Delta\phi + \frac{1}{\epsilon^2}G(\phi),$$

$$(3.6) \qquad\qquad \frac{d}{dt}A(\phi) = 0,$$

$$(3.7) \qquad\qquad \frac{d}{dt}H(\phi) = 0,$$

where $M$ is the mobility constant. The boundary conditions can be either one of the following two types:

$$(3.8) \qquad\qquad (i)\ \text{periodic; or}\ (ii)\ \partial_{\mathbf{n}}\phi|_{\partial\Omega} = \partial_{\mathbf{n}}w|_{\partial\Omega} = 0,$$

where $\mathbf{n}$ is the unit outward normal on the boundary $\partial\Omega$.

LEMMA 3.1. *The system* (3.3)–(3.7) *with* (3.8) *admits the following energy dissipative law:*

$$(3.9) \qquad\qquad \frac{d}{dt}E_b(\phi) = -M(\mu, \mu).$$

*Proof.* Taking the $L^2$ inner products of (3.3) with $\mu$, and of (3.4) with $\phi_t$ and of (3.5) with $w$, integrating by parts, and summing up the results, noticing that $(1, \phi_t) = \frac{d}{dt}A(\phi) = 0$ and $(\frac{\delta H}{\delta\phi}, \phi_t) = \frac{d}{dt}H(\phi) = 0$, we obtain the energy dissipative law. □

To simplify the presentation, we shall only construct a scheme using the third approach in the last section, since it is simpler than the second approach while maintaining unconditional energy stability. Obviously, schemes based on other approaches can be constructed similarly. We rewrite the blending energy as

$$(3.10) \quad \begin{aligned} E_b(\phi) &= \frac{\epsilon}{2}\int_\Omega |\Delta\phi|^2 d\boldsymbol{x} + \frac{\epsilon}{2}\int_\Omega \frac{6}{\epsilon^2}\phi^2|\nabla\phi|^2 + \frac{1}{\epsilon^4}(G(\phi))^2 - \frac{2}{\epsilon^2}|\nabla\phi|^2 d\boldsymbol{x} \\ &= \frac{\epsilon}{2}\int_\Omega |\Delta\phi|^2 d\boldsymbol{x} + \int_\Omega Q(\phi)d\boldsymbol{x}, \end{aligned}$$

where $Q(\phi) = \frac{\epsilon}{2}\{\frac{6}{\epsilon^2}\phi^2|\nabla\phi|^2 + \frac{1}{\epsilon^4}(G(\phi))^2 - \frac{2}{\epsilon^2}|\nabla\phi|^2\}$. The key in the second and third approaches is to introduce a Lagrange multiplier $\eta(t)$ to deal with the nonlinear part of the energy $Q(\phi)$ and reformulate (3.3)–(3.7) as

$$(3.11) \qquad \phi_t = -M\mu,$$

$$(3.12) \qquad \mu = \epsilon\Delta^2\phi + \eta(t)\frac{\delta Q}{\delta\phi} + \gamma(t) + \lambda(t)\frac{\delta H}{\delta\phi},$$

$$(3.13) \qquad \frac{d}{dt}\int_\Omega Q(\phi)d\boldsymbol{x} = \eta(t)\left(\frac{\delta Q}{\delta\phi}, \phi_t\right) + \lambda(t)\left(\frac{\delta H}{\delta\phi}, \phi_t\right),$$

$$(3.14) \qquad \frac{d}{dt}A(\phi) = 0,$$

$$(3.15) \qquad \frac{d}{dt}H(\phi) = 0.$$

Note that the last term in (3.13) is zero. We added this term which is essential in constructing efficient energy stable schemes.

**3.2. A second-order scheme based on the third approach.** As an example, we construct below a second-order (BDF2) scheme for system (3.11)–(3.15) based on the third approach:

$$(3.16) \qquad \frac{3\phi^{n+1} - 4\phi^n + \phi^{n-1}}{2\delta t} = -M\mu^{n+1},$$

$$(3.17) \qquad \mu^{n+1} = \epsilon\Delta^2\phi^{n+1} + \eta^{n+1}\left(\frac{\delta Q}{\delta\phi}\right)^{*,n+1} + \gamma^{n+1} + \lambda^{n+1}\left(\frac{\delta H}{\delta\phi}\right)^{*,n+1},$$

$$(3.18) \qquad \int_\Omega 3Q(\phi^{n+1}) - 4Q(\phi^n) + Q(\phi^{n-1})d\boldsymbol{x}$$

$$(3.19) \qquad\qquad = \eta^{n+1}\left(\left(\frac{\delta Q}{\delta\phi}\right)^{*,n+1}, 3\phi^{n+1} - 4\phi^n + \phi^{n-1}\right)$$

$$\qquad\qquad\qquad + \lambda^{n+1}\left(\left(\frac{\delta H}{\delta\phi}\right)^{*,n+1}, 3\phi^{n+1} - 4\phi^n + \phi^{n-1}\right),$$

$$(3.20) \qquad \int_\Omega \bar{\phi}^{n+1}d\boldsymbol{x} = \int_\Omega \phi^0 d\boldsymbol{x},$$

$$(3.21) \qquad H(\bar{\phi}^{n+1}) = H(\phi^0),$$

where $g^{*,n+1} = 2g^n - g^{n-1}$ for any sequence $\{g^n\}$, and $\bar{\phi}^{n+1}$ is defined in (3.24) below during the solution procedure.

Setting

$$(3.22) \qquad \phi^{n+1} = \phi_1^{n+1} + \eta^{n+1}\phi_2^{n+1} + \gamma^{n+1}\phi_3^{n+1} + \lambda^{n+1}\phi_4^{n+1}$$

in (3.16)–(3.17) and eliminating $\mu^{n+1}$, we find that $\{\phi_i^{n+1}\}$ can be determined by

$$(3.23) \qquad \left(\frac{1}{2\delta t} + M\epsilon\Delta^2\right)\phi_i^{n+1} = g_i, \quad i = 1, 2, 3, 4,$$

with $g_i$ to be known functions from previous steps. Once $\{\phi_i^{n+1}, \ i = 1, 2, 3, 4\}$ are known, we define

$$(3.24) \qquad \bar{\phi}^{n+1} = \phi_1^{n+1} + \phi_2^{n+1} + \gamma^{n+1}\phi_3^{n+1} + \lambda^{n+1}\phi_4^{n+1}.$$

Note that $\bar{\phi}^{n+1}$ is still as good an approximation to $\phi|_{t^{n+1}}$ as $\phi^{n+1}$ since $\eta^{n+1}$ is a second-order approximation to 1.

We can then determine the three Lagrange multipliers as follows:

- Plugging (3.24) into (3.20), we obtain a linear relation between $\gamma^{n+1}$ and $\lambda^{n+1}$.
- Plugging (3.24) into (3.21) and using the linear relation between $\gamma^{n+1}$ and $\lambda^{n+1}$, we obtain a nonlinear algebraic equation for $\lambda^{n+1}$ which can be solved a Newton iteration using an initial guess obtained by a linear scheme as in section 2.1.
- With $\gamma^{n+1}$ and $\lambda^{n+1}$ known, determine $\eta^{n+1}$ by plugging (3.22) into (3.19) and solve the resulting nonlinear algebraic equation with the initial guess 1.

Hence, the above scheme can be implemented very efficiently. As for the stability, we have the following result.

THEOREM 3.1. *Let* $\{\phi^k, \mu^k, \lambda^k, \eta^k, \gamma^k\}$ *be a solution of the scheme* (3.16)–(3.20). *Then, the following energy law is satisfied unconditionally for all n:*

$$E_b^{n+1} - E_b^n \le -\delta t M \|\mu^{n+1}\|^2,$$

*where*

$$(3.25) \quad E_b^{n+1} = \frac{\epsilon}{4}(\|\Delta\phi^{n+1}\|^2 + \|\Delta(2\phi^{n+1} - \phi^n)\|^2) + \frac{1}{2}\int_\Omega 3Q(\phi^{n+1}) - Q(\phi^n)\, d\boldsymbol{x},$$

*which is a second-order approximation to the original free energy* $E_b(\phi)$ *at* $t^{n+1}$.

*Proof.* Taking the inner product of (3.16) with $2\delta t\mu^{n+1}$, we derive

$$(3.26) \qquad (3\phi^{n+1} - 4\phi^n + \phi^{n-1}, \mu^{n+1}) = -2\delta t M \|\mu^{n+1}\|^2.$$

Due to (3.20), we have

$$(3.27) \qquad (1, 3\phi^{n+1} - 4\phi^n + \phi^{n-1}) = 0.$$

Taking the inner product of (3.17) with $3\phi^{n+1} - 4\phi^n + \phi^{n-1}$ and using equality (3.27) and (3.19), we derive

$$(3.28) \quad \begin{aligned} (3\phi^{n+1} - 4\phi^n + \phi^{n-1}, \mu^{n+1}) &= (\epsilon\Delta^2\phi^{n+1}, 3\phi^{n+1} - 4\phi^n + \phi^{n-1}) \\ &\quad + \int_\Omega 3Q(\phi^{n+1}) - 4Q(\phi^n) + Q(\phi^{n-1}) d\boldsymbol{x}. \end{aligned}$$

Using the identity

$$(3.29) \quad \begin{aligned} 2(a^{n+1}, 3a^{n+1} - 4a^n + a^{n-1}) &= \|a^{n+1}\|^2 - \|a^n\|^2 + \|a^{n+1} - 2a^n + a^{n-1}\|^2 \\ &\quad + \|2a^{n+1} - a^n\|^2 - \|2a^n - a^{n-1}\|^2, \end{aligned}$$

we have

$$\begin{aligned} (\epsilon\Delta^2\phi^{n+1}, 3\phi^{n+1} - 4\phi^n + \phi^{n-1}) &= \frac{\epsilon}{2}(\|\Delta\phi^{n+1}\|^2 - \|\Delta\phi^n\|^2 + \|\Delta(2\phi^{n+1} - \phi^n)\|^2 \\ &\quad - \|\Delta(2\phi^n - \phi^{n-1})\|^2 + \|\Delta(\phi^{n+1} - 2\phi^n + \phi^{n-1})\|^2). \end{aligned}$$

Combining the above equalities and dropping some unnecessary terms, we arrive at the desired result. $\square$

**4. A multicomponent system with multiple constraints.** We consider in this section a norm-preserving model for optimal partition written in the form of gradient flow. It is a multicomponent system with multiple constraints.

**4.1. The model.** The optimal partition problem can be described by a norm-preserving gradient dynamics [11]. Given a positive integer $m$ and a small parameter $\epsilon$, the total free energy is given by

$$(4.1) \qquad E(\boldsymbol{\phi}) = \int_\Omega \left( \frac{1}{2} |\nabla \boldsymbol{\phi}|^2 + \boldsymbol{F}(\boldsymbol{\phi}) \right) d\boldsymbol{x},$$

where $\boldsymbol{\phi} \in \mathbb{X}^m$ ($\mathbb{X} \subset H^1(\Omega)$ with suitable boundary conditions) is a vector valued function satisfying the norm constraint

$$(4.2) \qquad H_j(\phi) := \int_\Omega |\phi_j|^2 d\boldsymbol{x} = 1, \quad j = 1, 2, \ldots, m,$$

$\boldsymbol{F}$ represents interaction potential of each partition

$$(4.3) \qquad \boldsymbol{F}(\boldsymbol{\phi}) = \frac{1}{\epsilon^2} \sum_{i=1}^m \sum_{j<i} \phi_i^2 \phi_j^2.$$

We shall enforce the normalization conditions (4.2) by introducing $j$ Lagrange multipliers. The corresponding gradient flow reads

$$(4.4) \qquad \partial_t \phi_j = - \mu_j,$$

$$(4.5) \qquad \mu_j = - \Delta \phi_j - \lambda_j(t) \phi_j + \frac{\delta \boldsymbol{F}}{\delta \phi_j},$$

$$(4.6) \qquad \frac{d}{dt} \int_\Omega |\phi_j(x,t)|^2 d\boldsymbol{x} = 0, \quad j = 1, 2, \ldots, m,$$

with initial condition satisfying $\int_\Omega |\phi_j(x,0)|^2 d\boldsymbol{x} = 1$ and boundary conditions being

$$(4.7) \qquad \text{either (i) periodic or (ii) } \boldsymbol{\phi}|_{\partial\Omega} = 0.$$

LEMMA 4.1. *The system* (4.4)–(4.6) *with* (4.7) *admits the following energy dissipative law:*

$$(4.8) \qquad \frac{d}{dt} E(\boldsymbol{\phi}) = - M \int_\Omega \sum_{j=1}^m \mu_j^2 d\boldsymbol{x}.$$

*Proof.* Taking the inner products of (4.4) with $\mu_j$ and of (4.5) with $\partial_t \phi_j, j = 1, 2, \ldots, m$, noticing the equality (4.6), integrating by parts, and summing up all the relations, we obtain the desired result. □

Again the key for the second and third approaches is to introduce a Lagrange multiplier to deal with the nonlinear term and rewrite the system (4.4)–(4.6) as

$$(4.9) \qquad \partial_t \phi_j = - \mu_j,$$

$$(4.10) \qquad \mu_j = - \Delta \phi_j - \lambda_j(t) \phi_j + \eta(t) \frac{\delta \boldsymbol{F}}{\delta \phi_j},$$

$$(4.11) \qquad \frac{d}{dt} \int_\Omega \boldsymbol{F}(\boldsymbol{\phi}) d\boldsymbol{x} = \sum_{j=1}^m \eta(t) \left( \frac{\delta \boldsymbol{F}}{\delta \phi_j}, \partial_t \phi_j \right) + \sum_{j=1}^m \lambda_j(t)(\phi_j, \partial_t \phi_j),$$

$$(4.12) \qquad \frac{d}{dt} \int_\Omega |\phi_j(x,t)|^2 d\boldsymbol{x} = 0, \quad j = 1, \ldots m.$$

Note that we added the last term in (4.11) which is zero but is essential in constructing energy stable schemes below.

**4.2. A second-order scheme based on the third approach.** As an example, we construct below a second-order (BDF2) scheme for the system (4.4)–(4.6) based on the third approach.

We can construct a second-order scheme based on system (4.9)–(4.11).

For $j = 1, 2, \ldots, m$,

$$(4.13) \qquad \frac{3\phi_j^{n+1} - 4\phi_j^n + \phi_j^{n-1}}{2\delta t} = -\mu_j^{n+1},$$

$$(4.14) \qquad \mu_j^{n+1} = -\Delta\phi_j^{n+1} - \lambda_j^{n+1}\phi_j^{\star,n+1} + \eta^{n+1} f(\phi_j^{\star,n+1}),$$

$$(4.15) \qquad \int_\Omega 3\boldsymbol{F}(\boldsymbol{\phi}^{n+1}) - 4\boldsymbol{F}(\boldsymbol{\phi}^n) + \boldsymbol{F}(\boldsymbol{\phi}^{n-1}) d\boldsymbol{x}$$

$$(4.16) \qquad = \sum_{j=1}^m \left\{ \left( \eta^{n+1} \left( \frac{\delta \boldsymbol{F}}{\delta \phi_j} \right)^{\star,n+1}, 3\phi_j^{n+1} - 4\phi_j^n + \phi_j^{n-1} \right) \right.$$

$$\left. + (\lambda_j^{n+1}\phi_j^{\star,n+1}, 3\phi_j^{n+1} - 4\phi_j^n + \phi_j^{n-1}) \right\},$$

$$(4.17) \qquad \int_\Omega |\bar{\phi}_j^{n+1}|^2 d\boldsymbol{x} = \int_\Omega |\phi_j^0|^2 d\boldsymbol{x},$$

where $g^{\star,n+1} = 2g^n - g^{n-1}$ for any sequence $\{g^n\}$, and $\bar{\phi}_j^{n+1}$ is defined in (4.20) below during the solution procedure.

Setting

$$(4.18) \qquad \phi_j^{n+1} = \psi_{0,j}^{n+1} + \lambda_j^{n+1}\psi_{1,j}^{n+1} + \eta^{n+1}\psi_{2,j}^{n+1}, \quad j = 1, 2, \ldots, m,$$

and plugging the above into (4.13)–(4.14), we can determine $\psi_{0,j}^{n+1}$, $\psi_{1,j}^{n+1}$, and $\psi_{2,j}^{n+1}$ by solving decoupled linear equations

$$(4.19) \qquad \left( \frac{3}{2\delta t} - \Delta \right) \psi_{k,j}^{n+1} = g_{k,j}, \quad k = 0, 1, 2, \ j = 1, 2, \ldots, m,$$

where $\{g_{k,j}\}$ are known functions from the previous steps. Then we define

$$(4.20) \qquad \bar{\phi}_j^{n+1} = \psi_{0,j}^{n+1} + \lambda_j^{n+1}\psi_{1,j}^{n+1} + \psi_{2,j}^{n+1}, \quad j = 1, 2, \ldots, m.$$

Note that $\bar{\phi}_j^{n+1}$ is still as good an approximation to $\phi_j|_{t^{n+1}}$ as $\phi_j^{n+1}$ since $\eta^{n+1}$ is a second-order approximation to 1.

Finally, we determine $\{\lambda_j^{n+1}\}$ and $\eta^{n+1}$ as follows:
- Plug (4.20) into (4.17), we obtain, for each $j$, a quadratic algebraic equation for $\lambda_j^{n+1}$ which can be directly solved.
- With $\{\lambda_j^{n+1}\}$ known, we plug (4.18) into (4.16) to obtain a nonlinear algebraic equation for $\eta^{n+1}$, and we solve the nonlinear algebraic equation by a Newton iteration with 1 as initial condition.

Hence, the above scheme can be efficiently implemented. As for the stability, we have the following result.

THEOREM 4.1. *Let* $\{\phi^k, \mu^k, \eta^k, \lambda_j^k \, (1 \leq j \leq m)\}$ *be a solution of the scheme* (4.13)–(4.17). *Then, the following energy law is satisfied unconditionally for all n:*

$$E^{n+1} - E^n \leq -\delta t \sum_{j=1}^{m} \|\mu_j^{n+1}\|^2,$$

*where*

$$(4.21) \quad E^{n+1} = \frac{1}{4}(\|\nabla \phi^{n+1}\|^2 + \|\nabla(2\phi^{n+1} - \phi^n)\|^2) + \frac{1}{2}\int_\Omega 3\boldsymbol{F}(\phi^{n+1}) - \boldsymbol{F}(\phi^n)d\boldsymbol{x},$$

*which is a second-order approximation to the original free energy* $E(\boldsymbol{\phi})$ *at* $t^{n+1}$.

*Proof.* Taking the inner product of (4.13) with $2\delta t \mu_j^{n+1}$, we derive

$$(4.22) \qquad\qquad (3\phi_j^{n+1} - 4\phi_j^n + \phi_j^{n-1}, \mu_j^{n+1}) = -2\delta t \|\mu_j^{n+1}\|^2.$$

Taking the inner product of (4.14) with $3\phi_j^{n+1} - 4\phi_j^n + \phi_j^{n-1}$, and summing up all these equations from $j = 1, 2, \ldots, m$, we obtain

$$\begin{aligned}
(4.23) \quad \sum_{j=1}^{m}(3\phi_j^{n+1} - 4\phi_j^n + \phi_j^{n-1}, \mu_j^{n+1}) = &\sum_{j=1}^{m}(\nabla\phi_j^{n+1}, \nabla(3\phi_j^{n+1} - 4\phi_j^n + \phi_j^{n-1})) \\
&+ \int_\Omega 3\boldsymbol{F}(\boldsymbol{\phi}^{n+1}) - 4\boldsymbol{F}(\boldsymbol{\phi}^n) + \boldsymbol{F}(\boldsymbol{\phi}^{n-1})d\boldsymbol{x}.
\end{aligned}$$

Combining all relations obtained above and using the identity (3.29), we obtain the desired result. $\qquad\square$

**5. Numerical results.** We present in this section some numerical experiments to compare the performance of different approaches and to validate their stability and convergence rates. In all numerical examples below, we assume periodic boundary conditions and use a Fourier spectral method in space. The computational domain is $[-\pi, \pi)^d$ with $d = 2, 3$.

**5.1. Validation and comparison.** We consider the phase field vesicle membrane model (3.3)–(3.7) with $\epsilon = \frac{6\pi}{128}$, $M = 1$, and use 128 modes in each direction in our Fourier spectral method so that the spatial discretization errors are negligible compared with time discretization error.

**5.1.1. Comparison of the three approaches.** We first investigate the performance of the three approaches proposed in section 2. We consider the two-dimensional (2D) phase field vesicle membrane model (3.3)–(3.7) and choose as initial condition two close-by circles given by

$$(5.1) \qquad \phi(x, y, 0) = \sum_{i=1}^{2} \tanh\left(\frac{r_i - \sqrt{(x - x_i)^2 + (y - y_i)^2}}{\sqrt{2}\epsilon}\right) + 1.$$

We define $(r_1, r_2) = (0.28\pi, 0.28\pi)$, $(x_1, x_2) = (0, 0)$ and $(y_1, y_2) = (0.35\pi, -0.35\pi)$. In the left of Figure 1, we plot the evolution of Lagrange multiplier $\lambda$ with respect to time by using BDF2 scheme of three numerical approaches. We observe that the three
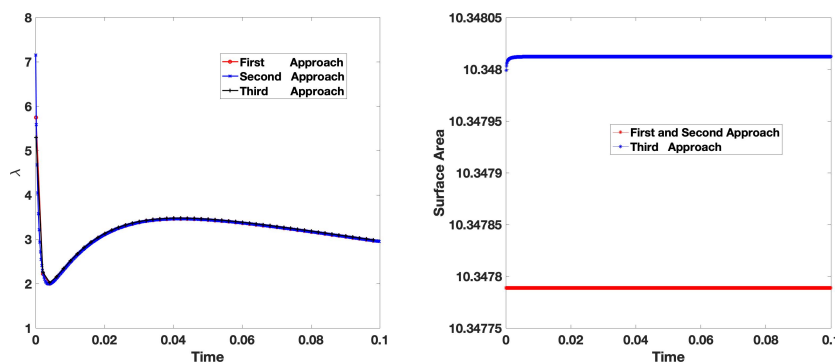
FIG. 1. *Left: Evolution of $\lambda$ by using three approaches with $\delta t = 10^{-4}$ for the first and third approaches while $\delta t = 10^{-5}$ for the second approach. Right: Evolution of the surface area.*

approaches lead to indistinguishable $\lambda$. However, we have to use a very small time step, $\delta t = 10^{-5}$, in the second approach for the Newton iteration to converge, while larger time steps can be used for the first and third approaches. On the other hand, we plot in the right of Figure 1 the evolution of the surface area by using the three approaches. We observe that the first and second approaches preserve exactly the surface area, while very small differences on $B(\phi)$ are observed by the third approach at several initial time steps, since the third approach only preserves $B(\bar{\phi})$ instead of $B(\phi)$.

The above results indicate that the first and third approaches are preferable over the second approach, since they allow larger time steps. Therefore, we shall only use the first and third approaches in the remaining simulations.

**5.1.2. Convergence rate.** We test the convergence rate of BDF2 schemes using first and third approaches for 2D phase field vesicle membrane model (3.3)–(3.7) with the initial condition

$$(5.2) \qquad \phi(x, y, 0) = \left( \frac{\sin(2x)\cos(2y)}{4} + 0.48 \right) \left( 1 - \frac{\sin^2(t)}{2} \right).$$

The reference solutions are obtained with a small time step $\delta t = 10^{-5}$ using the BDF2 schemes. In Figure 2, we plot the $L^\infty$ errors of $\phi$ between numerical solution and reference solution with different time steps. We observe that second-order convergence rates are achieved by both approaches.

**5.1.3. Comparison between the new approaches and the penalty approach in [7].** We now compare our Lagrange multiplier approach with the penalty approach developed in [7]. In the penalty approach, we introduce two penalty parameters $\gamma$ and $\eta$ and consider the total free energy

$$(5.3) \qquad E_{total}(\phi) = E_b(\phi) + \frac{1}{2\gamma}(A(\phi) - A(\phi|_{t=0}))^2 + \frac{1}{2\eta}(H(\phi) - H(\phi|_{t=0}))^2,$$

where $E_b(\phi)$, $A(\phi)$, and $H(\phi)$ are defined in (3.1) and (3.2). We observe that the penalty approach can only approximately preserve the constraints on $A(\phi)$ and $H(\phi)$, and very small penalty parameters have to be used if we want to preserve the constraints to a high accuracy. However, small penalty parameters will lead to stiff systems such
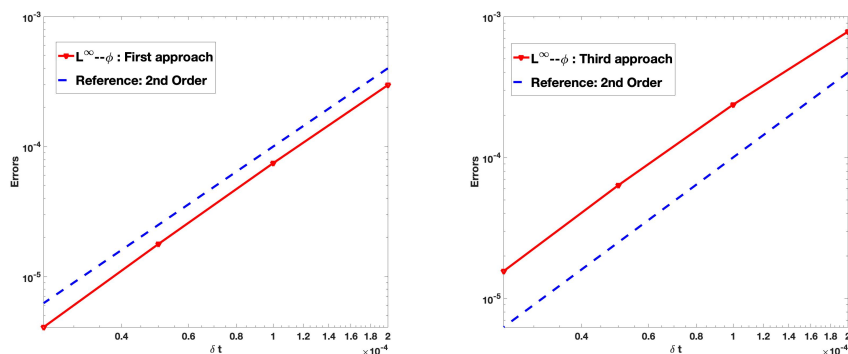
Fig. 2. *Convergence rate of BDF2 schemes by using the first and third approaches for 2D phase field vesicle membrane model* (3.3)–(3.7).

TABLE 1
*Largest time step allowed for MSAV scheme with various Penalty parameters $\gamma$ and $\eta$.*

| $\delta t$ allowed | $\gamma$ | $\eta$ |
|---|---|---|
| $2 \times 10^{-4}$ | $10^{-5}$ | $10^{-5}$ |
| $2 \times 10^{-4}$ | $10^{-6}$ | $10^{-6}$ |
| $1 \times 10^{-4}$ | $10^{-7}$ | $10^{-7}$ |
| $5 \times 10^{-5}$ | $10^{-8}$ | $10^{-8}$ |
| $2 \times 10^{-5}$ | $10^{-9}$ | $10^{-9}$ |
| $1 \times 10^{-5}$ | $10^{-10}$ | $10^{-10}$ |
| $2 \times 10^{-6}$ | $10^{-11}$ | $10^{-11}$ |
| $1 \times 10^{-6}$ | $10^{-12}$ | $10^{-12}$ |

that the MSAV approach proposed in [7] requires very small time steps to get accurate solutions. More precisely, we list the maximum allowable time step in Table 1 for the MSAV scheme for the 2D phase field vesicle membrane model by using the penalty approach. We observe that the maximum allowable time step behaves like $\min(\sqrt{\gamma}, \sqrt{\eta})$. On the other hand, the new Lagrangian multiplier approach is more efficient than the MSAV approach at each time step and allows much larger time steps.

Next, we simulate the 3D phase field vesicle membrane model with the first approach proposed in this paper and the MSAV approach in [7]. We take the initial condition as

$$(5.4) \qquad \phi(x,y,z,0) = \sum_{i=1}^{4} \tanh\left(\frac{r_i - \sqrt{(x-x_i)^2 + (y-y_i)^2 + (z-z_i)^2}}{\sqrt{2}\epsilon}\right) + 3,$$

where $r_i = \frac{\pi}{6}$, $x_i = 0$, $(y_1, y_2, y_3, y_4) = (\frac{\pi}{4}, -\frac{\pi}{4}, \frac{3\pi}{4}, -\frac{3\pi}{4})$, and $z_i = 0$ for $i = 1, 2, 3, 4$.

In Figure 3, we plot the evolution of the volume difference and surface area difference by the MSAV scheme in [7] with penalty parameter $\gamma = \eta = 10^{-3}$ and by the BDF2 scheme of first approach using $\delta t = 2 \times 10^{-4}$. We observe that both the volume and surface area are preserved exactly by the BDF2 scheme of first approach while only approximately for the MSAV scheme using the penalty approach.
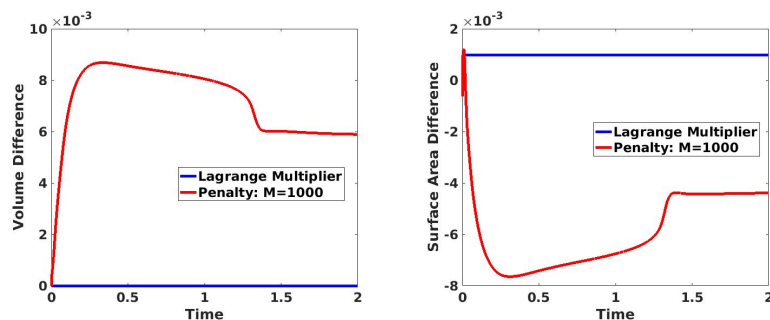
FIG. 3. *Evolution of the volume and surface area differences by the MSAV scheme* $\gamma = \eta = 10^{-3}$ *and the BDF2 scheme of first approach with* $\delta t = 2 \times 10^{-4}$.
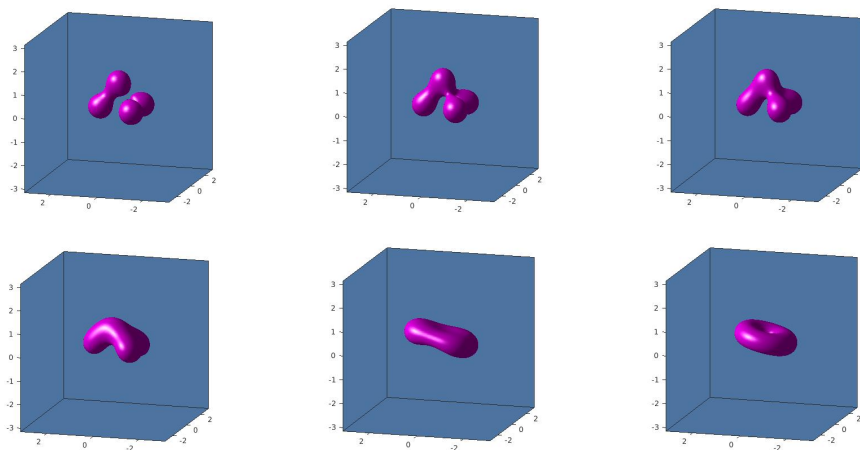


FIG. 4. *Collision of four 3D close-by spherical vesicles by using the BDF2 of first approach with the time step size* $\delta t = 2 \times 10^{-4}$. *Snapshots of isosurface of* $\phi$ *at* $t = 0.01, 0.02, 0.04, 0.2, 1, 2$.

In Figure 4, we present snapshots of isosurface of $\{\phi = 0\}$ at different times by using the BDF2 scheme of first approach. It is observed that the final steady state is the same as that reported in [7] using the penalty approach. We also plot in Figure 5 energy curves of different approaches which are indistinguishable in all cases.

**5.2. Additional simulations of 3D vesicle membrane model.** In order to further demonstrate the accuracy and robustness of our new Lagrangian multiplier approach, we perform some additional simulations of the 3D vesicle membrane model. As the first example, we set four close-by spheres as the initial profile which is formulated as

$$(5.5) \qquad \phi(x, y, z, 0) = \sum_{i=1}^{4} \tanh\left( \frac{r_i - \sqrt{(x - x_i)^2 + (y - y_i)^2 + (z - z_i)^2}}{\sqrt{2}\epsilon} \right) + 3,$$

where $r_i = \frac{\pi}{6}$, $x_i = 0$, $(y_1, y_2, y_3, y_4) = (\frac{\pi}{4}, -\frac{\pi}{4}, \frac{3\pi}{4}, -\frac{3\pi}{4})$, and $z_i = 0$ for $i = 1, 2, 3, 4$. In Figure 6, we plot several snapshots of the isosurface $\{\phi = 0\}$ by using the BDF2
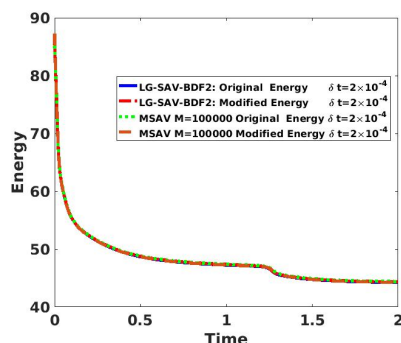
FIG. 5. *Energy evolutions with different approaches using the initial condition* (5.4).
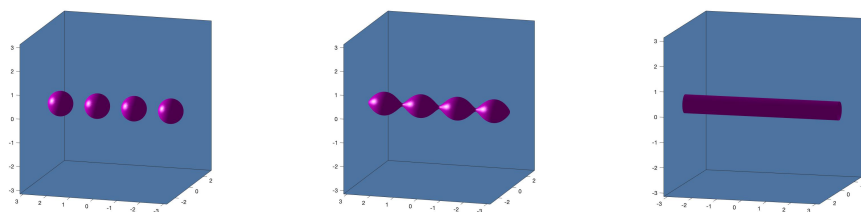


FIG. 6. *Collision of four close-by spherical vesicles by using the third approach with time step size $\delta t = 1 \times 10^{-4}$. Snapshots of isosurface of $\{\phi = 0\}$ at $t = 0, 0.02, 1$.*

scheme of the third approach with $\delta t = 10^{-4}$. It is observed that initially separated four spheres connect with each other at $t = 0.02$ and gradually merge into a cylinder shape at $t = 1$. This is consistent with results in [13].

As the second example, we start with a more complicated initial condition given by

$$(5.6) \qquad \phi(x, y, z, 0) = \sum_{i=1}^{6} \tanh \left( \frac{r_i - \sqrt{(x - x_i)^2 + (y - y_i)^2 + (z - z_i)^2}}{\sqrt{2}\epsilon} \right) + 5,$$

where $r_i = \frac{\pi}{6}$, $z_i = 0$ for $i = 1, 2, \ldots, 6$ $(x_1, x_2, x_3, x_4, x_5, x_6) = (-\frac{\pi}{4}, \frac{\pi}{4}, 0, \frac{\pi}{2}, -\frac{\pi}{2}, 0)$, and $(y_1, y_2, y_3, y_4, y_5, y_6) = (-\frac{\pi}{4}, -\frac{\pi}{4}, \frac{\pi}{4}, \frac{\pi}{4}, \frac{\pi}{4}, -\frac{3\pi}{4})$.

In Figure 7, we plot snapshots of isosurface $\{\phi = 0\}$ at $t = 0, 0.01, 0.02, 0.2, 0.5, 2$ by using the BDF2 scheme of the first approach. We observe from this figure that the initially separated spheres connect with each other in a short time and eventually merge into a big vesicle. The shape of the final steady state is consistent with simulations in [13].

We also plot, in Figure 8, the evolution of Lagrange multiplier $\lambda$ for these two examples. We observe that the Lagrange multiplier $\lambda$ will change rapidly at the begining and gradually settle down to a steady state value. We also observe that $\lambda$ can become negative.

**5.3. Optimal partition model.** We present below numerical experiments for the optimal partition problem (4.4)–(4.6). In [11], simulations are performed with Dirichlet boundary conditions. While the algorithms presented in the previous section
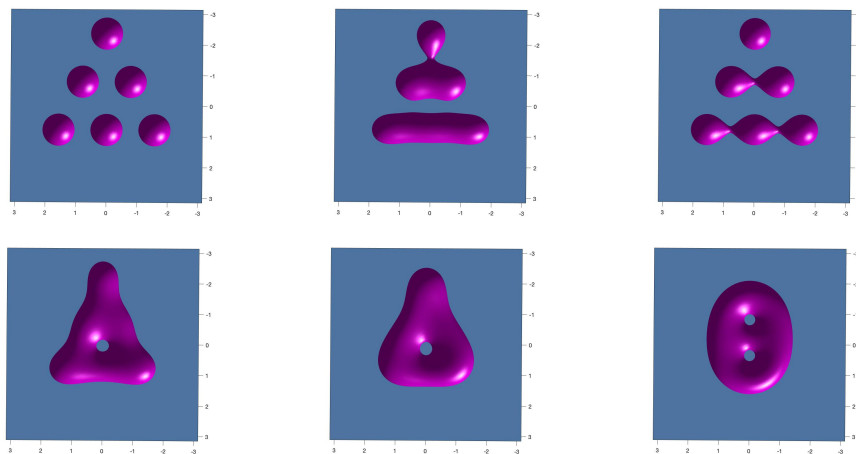
FIG. 7. *Collision of six close-by spherical vesicles by using the first approach with time step size* $\delta t = 1 \times 10^{-4}$. *Snapshots of isosurface of* $\{\phi = 0\}$ *at* $t = 0, 0.01, 0.02, 0.2, 0.5, 2$.
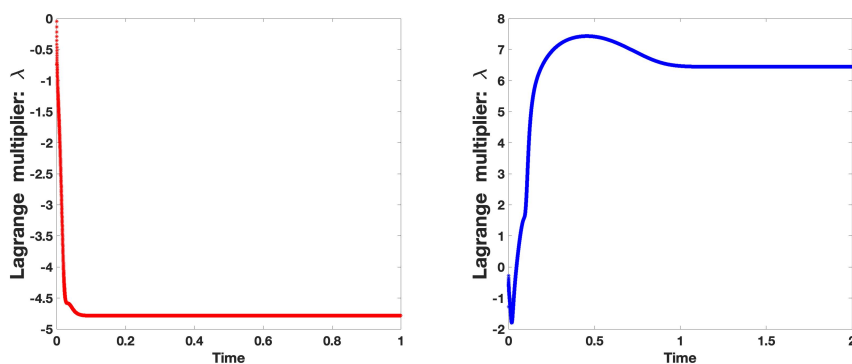


FIG. 8. *Evolution of Lagrange multiplier* $\lambda$ *for the examples in Figures* 6 *and* 7.

apply to both periodic and Dirichlet boundary conditions, for the sake of simplicity and comparison, we shall consider the periodic boundary condition with the Fourier spectral method is adopted to discretize the space variables in the computational domain $\Omega = [-\pi, \pi)^2$. In all computations, we use $128^2$ Fourier modes with interfacial width parameter $\epsilon = 0.01$. To better visualize the subdomain evolution, we assign an integer valued marker function $\chi_i$ which equals to $i$ in the region $i$, and $\chi_i = 0$ in other regions. The initial condition for $\phi_i$ is set to be the marker function $\chi_i$. The BDF2 scheme of the first approach with time step $\delta t = 10^{-5}$ is used for all examples below.

For the first example, we take $m = 4$ with four connected quadrilaterals as the initial configuration. In Figure 9, the evolutions of the phase configuration at various times are depicted. We observe that patterns in the partition gradually evolve into hexagonal patterns as the final steady state.
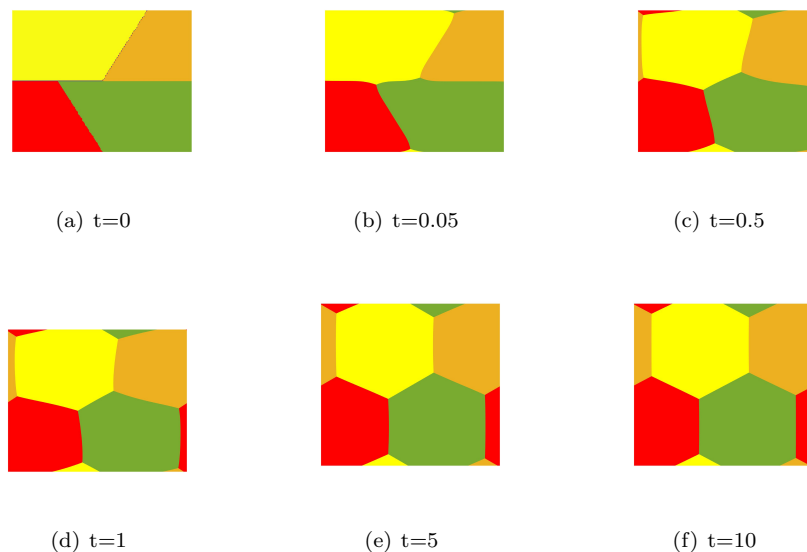
(a) t=0          (b) t=0.05          (c) t=0.5

(d) t=1          (e) t=5          (f) t=10

FIG. 9. *A 4-subdomain partition: initial partition and subdomains at times* $t = 0, 0.05, 0.5, 1, 5, 10$ *computed by the BDF2 scheme of the first approach with* $\delta t = 1 \times 10^{-5}$.
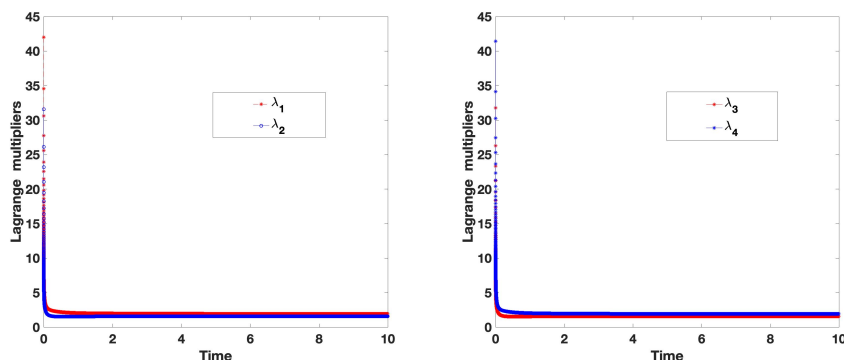


FIG. 10. *Evolution of Lagrange multipliers* $\lambda_1, \lambda_2$ *and* $\lambda_3, \lambda_4$ *with respect to time for 4-subdomain partition in Figure* 9.

For the optimal partition problem, it is shown in [4] that all Lagrange multipliers are positive and will decay with time. In Figure 10, we plot evolutions of the four Lagrange multipliers and observe that they are indeed positive and decay with time.

Next, we increase the numbers of partitions to $m = 8$ and plot in Figure 11 the evolutions of the phase configuration at various times. We observe that the partition eventually evolves into a honeycomb shape with mostly hexagonal patterns. Similar behaviors are observed with $m = 10$ as shown in Figure 12.

These numerical results are qualitatively consistent with the numerical simulations presented in [11], where the Dirichlet boundary condition was used.
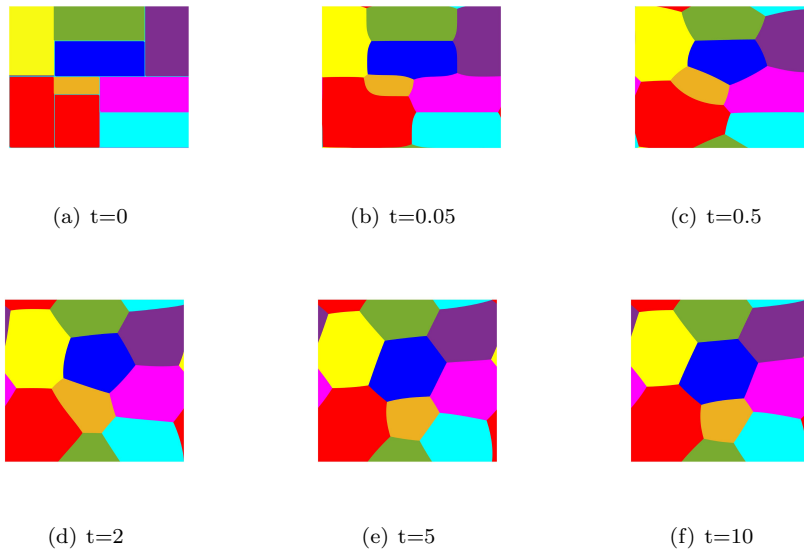
(a) t=0                     (b) t=0.05                    (c) t=0.5



(d) t=2                     (e) t=5                       (f) t=10

FIG. 11.    *An 8-subdomain partition:  initial partition and subdomains at times t =
0, 0.05, 0.5, 2, 5, 10 computed by the BDF2 scheme of the first approach with $\delta t = 1 \times 10^{-5}$.*



(a) t=0                     (b) t=0.05                    (c) t=0.5



(d) t=2                     (e) t=5                       (f) t=10

FIG. 12.    *A 10-subdomain partition:  initial partition and subdomains at times t =
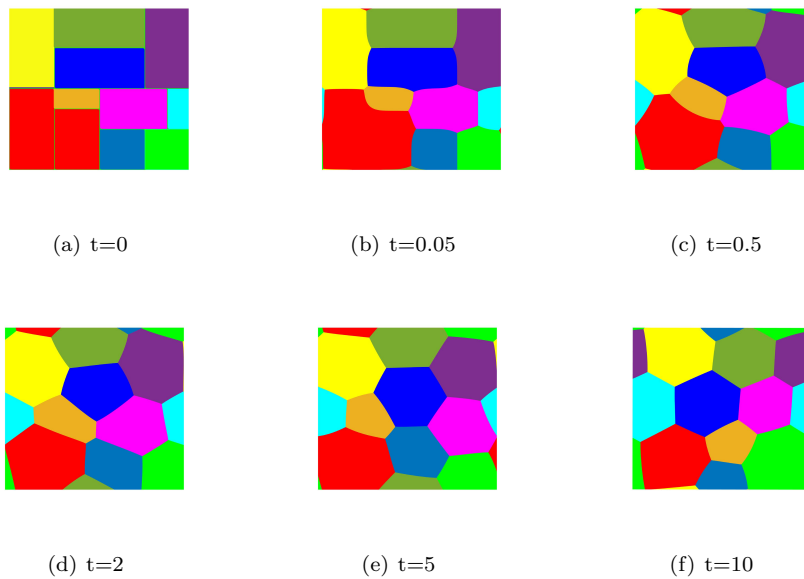0, 0.05, 0.5, 2, 5, 10 computed by the BDF2 scheme of the first approach with $\delta t = 1 \times 10^{-5}$.*

**6. Concluding remarks.** How to construct efficient numerical schemes for gra-
dient flows with global constraints is a challenging task. The popular penalty approach
may lead to very stiff systems that are difficult to solve, while a direct implementation

of the Lagrangian multiplier approach leads to nonlinear systems to solve at each time step. We developed several efficient numerical schemes which can preserve exactly the constraints for gradient flows with global constraints by combining the SAV approach with the Lagrangian multiplier approach. These schemes are as efficient as the SAV schemes for unconstrained gradient flows, i.e., only require solving linear equations with constant coefficients at each time step plus an additional nonlinear algebraic system which can be solved at negligible cost, and preserve exactly the constraints for constrained gradient flows. Moreover, the second and third approaches lead to schemes which are unconditionally energy stable. And the Lagrangian multipliers in the third approach can be determined sequentially, as opposed to coupled together in the second approach, making it more robust and efficient than the second approach.

We presented ample numerical results to compare the three approaches with the penalty approach. Our numerical results indicate that the proposed approaches can achieve accurate results and preserve exactly the constraints with larger time steps than those allowed in the penalty approach. And the first and third approaches are more robust and efficient than the second approach.

Although we considered only time discretization schemes in this paper, they can be combined with any consistent finite dimensional Galerkin type approximations in practice, since the stability proofs are all based on variational formulations with all test functions in the same space as the trial functions.

We would like to point out that we only provided formal stability results for the schemes presented in this paper, in the sense that we did not address the existence and uniqueness for the nonlinear algebraic systems involved in these schemes in the neighborhood of the exact solutions. A rigorous analysis for the well posedness and error estimates of these schemes is a subject of future study.

## REFERENCES

[1] U. M. ASCHER AND L. R. PETZOLD, *Computer Methods for Ordinary Differential Equations and Differential-algebraic Equations*, SIAM, Philadelphia, 1998.

[2] W. BAO AND Q. DU, *Computing the ground state solution of Bose–Einstein condensates by a normalized gradient flow*, SIAM J. Sci. Comput., 25 (2004), pp. 1674–1697, https://doi.org/10.1137/S1064827503422956.

[3] K. E. BRENAN, S. L. CAMPBELL, AND L. R. PETZOLD, *Numerical Solution of Initial-value Problems in Differential-algebraic Equations*, Classics in Appl. Math. 14, SIAM, Philadelphia, 1996.

[4] L. CAFFARELLI AND F. LIN, *An optimal partition problem for eigenvalues*, J. Sci. Comput., 31 (2007), pp. 5–18, https://doi.org/10.1007/s10915-006-9114-8.

[5] L. CAFFARELLI AND F. LIN, *Nonlocal heat flows preserving the l2 energy*, Discrete Contin. Dyn. Syst., 23 (2009), pp. 49–64, https://doi.org/10.3934/dcds.2009.23.49.

[6] Q. CHENG, C. LIU, AND J. SHEN, *A New Lagrange Multiplier Approach for Gradient Flows*, https://arxiv.org/abs/1911.08336, 2019.

[7] Q. CHENG AND J. SHEN, *Multiple scalar auxiliary variable (MSAV) approach and its application to the phase-field vesicle membrane model*, SIAM J. Sci. Comput., 40 (2018), pp. A3982–A4006, https://doi.org/10.1137/18M1166961.

[8] M. CONTI, S. TERRACINI, AND G. VERZINI, *An optimal partition problem related to nonlinear eigenvalues*, J. Funct. Anal., 198 (2003), pp. 160–196, https://doi.org/10.1016/S0022-1236(02)00105-2.

[9] Q. DU AND X. FENG, *The Phase Field Method for Geometric Moving Interfaces and Their Numerical Approximations*, preprint, arXiv:1902.04924, 2019.

[10] Q. DU, M. GUNZBURGER, R. B. LEHOUCQ, AND K. ZHOU, *Analysis and approximation of nonlocal diffusion problems with volume constraints*, SIAM Rev., 54 (2012), pp. 667–696, https://doi.org/10.1137/110833294.

[11] Q. Du and F. Lin, *Numerical approximations of a norm-preserving gradient flow and applications to an optimal partition problem*, Nonlinearity, 22 (2008), pp. 67–83, https://doi.org/10.1088/0951-7715/22/1/005.

[12] Q. Du, C. Liu, R. Ryham, and X. Wang, *Energetic variational approaches in modeling vesicle and fluid interactions*, Phys. D, 238 (2009), pp. 923–930, https://doi.org/10.1016/j.physd.2009.02.015.

[13] Q. Du, C. Liu, and X. Wang, *Simulating the deformation of vesicle membranes under elastic bending energy in three dimensions*, J. Comput. Phys., 212 (2006), pp. 757–777, https://doi.org/10.1016/j.jcp.2005.07.020.

[14] F. Guillén-González and G. Tierra, *Unconditionally energy stable numerical schemes for phase-field vesicle membrane model*, J. Comput. Phys., 354 (2018), pp. 67–85, https://doi.org/10.1016/j.jcp.2017.10.060.

[15] S. H. Jeong, G. H. Yoon, A. Takezawa, and D.-H. Choi, *Development of a novel phase-field method for local stress-based shape and topology optimization*, Computers & Structures, 132 (2014), pp. 84–98, https://doi.org/10.1016/j.compstruc.2013.11.004.

[16] X. Jing, J. Li, X. Zhao, and Q. Wang, *Second order linear energy stable schemes for Allen-Cahn equations with nonlocal constraints*, J. Sci. Comput., 80 (2019), pp. 500–537, https://doi.org/10.1007/s10915-019-00946-x.

[17] X. Jing and Q. Wang, *Linear second order energy stable schemes for phase field crystal growth models with nonlocal constraints*, Comput. Math. Appl., 79 (2020), pp. 764–788, https://doi.org/10.1016/j.camwa.2019.07.030.

[18] P. Kunkel and V. Mehrmann, *Differential-algebraic Equations: Analysis and Numerical Solution*, Vol. 2, European Mathematical Society, Zürich, 2006.

[19] K. Lee, K. Ahn, and J. Yoo, *A novel p-norm correction method for lightweight topology optimization under maximum stress constraints*, Computers & Structures, 171 (2016), pp. 18–30, https://doi.org/10.1016/j.compstruc.2016.04.005.

[20] J. Shen, J. Xu, and J. Yang, *The scalar auxiliary variable (SAV) approach for gradient flows*, J. Comput. Phys., 353 (2018), pp. 407–416, https://doi.org/10.1016/j.jcp.2017.10.021.

[21] J. Shen, J. Xu, and J. Yang, *A new class of efficient and robust energy stable schemes for gradient flows*, SIAM Rev., 61 (2019), pp. 474–506, https://doi.org/10.1137/17M1150153.

[22] J. Shen and X. Yang, *The IEQ and SAV approaches and their extensions for a class of highly nonlinear gradient flow systems*, Contemp. Math., 754 (2020), pp. 217–245.

[23] X. Wang, L. Ju, and Q. Du, *Efficient and stable exponential time differencing Runge–Kutta methods for phase field elastic bending energy models*, J. Comput. Phys., 316 (2016), pp. 21–38, https://doi.org/10.1016/j.jcp.2016.04.004.

[24] X. Yang, *Linear, first and second-order, unconditionally energy stable numerical schemes for the phase field model of homopolymer blends*, J. Comput. Phys., 327 (2016), pp. 294–316, https://doi.org/10.1016/j.jcp.2016.09.029.

[25] X. Yang and L. Ju, *Efficient linear schemes with unconditional energy stability for the phase field elastic bending energy model*, Comput. Methods Appl. Mech. Engrg., 315 (2017), pp. 691–712, https://doi.org/10.1016/j.cma.2016.10.041.

[26] X. Yang, J. Zhao, Q. Wang, and J. Shen, *Numerical approximations for a three components Cahn-Hilliard phase-field model based on the invariant energy quadratization method*, Math. Models Methods Appl. Sci., 27 (2017), pp. 1993–2030, https://doi.org/10.1142/S0218202517500373.

[27] Q. Zhuang and J. Shen, *Efficient SAV approach for imaginary time gradient flows with applications to one-and multi-component Bose-Einstein condensates*, J. Comput. Phys., 391 (2019), pp. 72–88, https://doi.org/10.1016/j.jcp.2019.06.043.